POLYMERIC OSTEOPONTIN EMPLOYS INTEGRIN α9β1 AS A RECEPTOR AND ATTRACTS NEUTROPHILS BY PRESENTING A *DE NOVO* BINDING SITE*

Norihisa Nishimichi[2,§], Fumiko Higashikawa[1,§,¶], Hiromi H. Kinoh[1], Yoshiko Tateishi[2], Haruo Matsuda[2], & Yasuyuki Yokosaki[1,3]

From [1]Cell-Matrix Frontier Laboratory, Biomedical Research Unit, Hiroshima University, 1-2-3 Kasumi, Minamiku, Hiroshima, 734-8551; [2]Laboratory of Immunobiology, Department of Molecular and Applied Biosciences, Graduate School of Biosphere Science, Hiroshima University, 1-4-4 Kagamiyama, Higashi-Hiroshima, 739-8528; [3]Health Administration Center, Hiroshima University, 1-7-1 Kagamiyama, Higashi-Hiroshima, 739-8521, Japan

Running title: Polymeric osteopontin attracts neutrophils binding to α9β1

Address correspondence to: Yasuyuki Yokosaki, M.D., Ph.D., Cell-Matrix Frontier Laboratory, Biomedical Research Building 216, Hiroshima University, 1-2-3 Kasumi, Minamiku, Hiroshima, 734-8551, Japan. Tel +81 82 257 1523; Fax +81 82 256 2376; E-mail: yokosaki@hiroshima-u.ac.jp

Osteopontin (OPN) is a cytokine and ligand for multiple members of the integrin family. OPN undergoes the *in vivo* polymerization catalyzed by cross-linking enzyme transglutaminase 2, which consequently increases the bioactivity through enhanced interaction with integrins. The integrin α9β1, highly expressed on neutrophils, binds to the sequence SVVYGLR only after intact OPN is cleaved by thrombin. The SVVYGLR sequence appears to be cryptic in intact OPN because α9β1 does not recognize intact OPN. Since transglutaminase 2-catalyzed polymers change their physical and chemical properties, we hypothesized the SVVYGLR site might also be exposed on polymeric OPN. As expected, α9β1 turned into a receptor for polymeric OPN, a result obtained by cell adhesion and migration assays with α9-transfected cells and by detection of direct binding of recombinant soluble α9β1 with colorimetry and surface plasmon resonance analysis. Because the N-terminal fragment of thrombin-cleaved OPN, a ligand for α9β1, has been reported to attract neutrophils, we next examined migration of neutrophils to polymeric OPN using time-lapse microscopy. Polymeric OPN showed potent neutrophil chemotactic activity, which was clearly inhibited by anti-α9β1 antibody. Unexpectedly, mutagenesis studies showed that α9β1 bound to polymeric OPN independently of the SVVYGLR sequence, and further SVVYGLR sequence of polymeric OPN was cryptic because SVVYGLR-specific antibody did not recognize polymeric OPN. These results demonstrate that polymerization of OPN generates a novel α9β1 binding site, and that interaction of this site with the α9β1 integrin is critical to the neutrophil chemotaxis induced by polymeric OPN.

Acidic phosphorylated secreted glycoprotein osteopontin (OPN), known as a cytokine, has multiple functions, including roles in tissue remodeling, fibrosis, mineralization, immunomodulation, inflammation, and tumor metastasis (1) (2) (3). OPN is also an integrin ligand. At least nine integrins can function as OPN receptors: α5β1, α8β1, αvβ1, αvβ3, αvβ5 (1) and αvβ6 (4) recognize the linear tripeptide RGD; and α9β1, α4β1 and α4β7 recognize the sequence, SVVYGLR (5) adjacent to RGD, but only after OPN has been cleaved by the protease, thrombin (Fig. 1).

The overlap of receptors for OPN does not necessarily mean that these integrins play redundant roles in cellular responses to OPN, since the patterns of integrin expression and utilization vary widely among cell types. In addition, interactions of different integrins with a single ligand can exert distinct effects on cell behavior in a single cell type. For example, we have previously reported that signals by ligation of αvβ3, αvβ6 or α9β1 to a single ligand, tenascin-C, differently affected cell adhesion, spreading and proliferation of the colon cancer cell line, SW480 (6). Furthermore, intact OPN, thrombin- or matrix metalloproteinase (MMP) -cleaved OPN, interact with distinct subsets of integrins and exhibit distinct effects on cell behavior (4, 7, 8). Collectively, some of the functional diversity of OPN could be attributed to this multiplicity of receptors and responses. We have recently shown that polymerization of OPN results in enhanced biological activity (9). We thus set out to determine whether polymerized OPN exerts its effects through unique interactions with integrins.

OPN is polymerized by transglutaminase 2 (TG2, EC 2.3.2.13) (10) that catalyzes formation of isopeptide cross-links be-

tween glutamine and lysine residues in substrate proteins (11) including OPN. Polymeric OPN has been identified *in vivo* in bone (12) and calcified aorta (13). We have previously reported that upon polymerization OPN displays increased integrin-binding accompanied by enhanced cell adhesion, spreading, migration, and focal contact formation (9). However, very little is known about how polymeric OPN induces its biological effects.

Integrin α9β1, highly expressed on neutrophils (14), does not act as a receptor for intact OPN but does bind to an N-terminal fragment of OPN (nOPN) that is generated by thrombin-cleavage (15), through the new C-terminal sequence, SVVYGLR. Protein polymerization can expose otherwise cryptic domains (16), so we hypothesized that the SVVYGLR site might be exposed upon polymerization and serve as a binding-site for α9β1. In the present study, we demonstrate that α9β1 is indeed a receptor for polymeric OPN, and that neutrophil migration induced by polymeric OPN is largely mediated by this interaction. However, mutational analysis and antibody studies demonstrate that this interaction does not involve the SVVYGLR site, suggesting the presence of *de novo* binding site in polymeric OPN.

Experimental procedures

Cells, antibodies and reagents- Mock- and α9-transfected human colon cancer cell line SW480 (17), and monoclonal antibody (mAb) specific for integrin α9β1 (Y9A2) (18) were provided by Dr. Dean Sheppard (UCSF, San Francisco, CA). FreeStyle 293F was obtained from Invitrogen. Anti-human integrin mAbs specific for α5β1 (JBS5), αvβ5 (P1F6) and β2 subunit (MEM48) were from Chemicon. Anti-OPN mAb 34E3 was from IBL (Takasaki, Japan). Mouse anti-V5 antibody was from Invitrogen. Horseradish peroxidase (HRP) -conjugated antibodies against mouse IgG and chicken IgY were form SouthernBiotech and BETHYL, respectively. TG2 was prepared and provided by Dr. Yuji Saito (Tokyo Institute of Technology, Yokohama, Japan) from guinea pig livers (19). Synthetic peptides were generated by Sigma-Aldrich Japan. Recombinant tenascin-C fragment of the third fibronectin type III repeat containing alanine substitution mutations within the RGD site (TNfn3RAA) was bacterially expressed as described (17). Vitronectin was from Chemicon.

Recombinant OPN proteins- As previously described (5), OPN proteins were expressed as glutathione S-transferase (GST)-fusion protein in *E. coli* with pGEX6P plasmid, and affinity-purified then cleaved from GST with PreScission protease (GE Healthcare). Human polymeric OPN was generated by incubation with guinea pig TG2 (9) and purified by anion-exchange chromatography (PerSeptive).

Antibody generation- Chicken mAb HUC750 was generated essentially as previously described (20). To obtain a reaction spectrum for both polymeric and intact OPN, chickens were immunized with polymeric OPN and the clone was screened with intact OPN. Briefly, after two month-old H-B15 inbred chickens were immunized, a phage-displayed library expressing immunoglobulin Fab fragments was constructed from each spleen of the chickens by fusing PCR-amplified immunoglobulin VH and VL regions. After the positive Fab phage clones were concentrated by a few rounds of panning, the Fab clone was finally reconstructed into chicken IgY form.

Site-directed mutagenesis- Performed with the QuickChange site-directed mutagenesis kit (Stratagene) as described (21).

Cell adhesion assay- Performed as described (17) with slight modifications. Briefly, cells were seeded into wells of MaxiSorp ELISA plates (Nunc) coated with substrate proteins at 4 °C for overnight and then incubated for 1 h at 37 °C. Attached cells were stained with 0.5% crystal violet and solubilized in 2% Triton X-100 for taking optical density at 595 nm.

Recombinant soluble α9β1- FreeStyle 293F cells were co-transfected with cDNAs encoding truncated α9 subunit cloned in pEF6/V5-His and β1 subunit in pcDNA3.1 (Invitrogen) lacking for the transmembrane and cytoplasmic domains. After screening with zeocin and neomycin, the V5-His-tagged α9β1 heterodimer was purified from culture supernatant by nickel chelate chromatography. For binding assay, 50 μl of recombinant soluble α9β1 in Tris-buffered saline containing 0.05 % tween 20 and 1 mM $MnCl_2$ was added at concentration of 2 μg/ml in each well of a ELISA plate coated with various OPN proteins or other substrates (50 μl at indicated concentration), and incubated for 60 min at 37 ºC. After washing off the unbound α9β1 with the same buffer, binding was assessed by colorimetric detection with anti-V5 antibody and secondary HRP-labeled antibody.

Affinity chromatography- Affinity chromatography was performed as recommended by the manufacturer. Briefly, TNfn3RAA was coupled to Sepharose gel (1 ml) in a HiTrap column (GE Healthcare) for 30 min at 25 °C. The affinity matrices were blocked with 0.5 M monoethanolamine, and then biotinylated recombinant soluble α9β1 was applied to the column, which had been equilibrated in column buffer (50 mM Tris-HCl, 50 mM NaCl, 1 mM $MnCl_2$). After the column was washed, bound protein was eluted with 20 mM EDTA. Column fractions were concentrated 20 times with Nanosep 30K ultrafiltration column (Pall) then loaded onto 7.5 % SDS-PAGE in a non-reducing condition. α9β1 on the gel was visualized with HRP-labeled avidin after transferred onto Immuno-Blot PVDF membrane (Bio-Rad).

Surface plasmon resonance (SPR) analysis- Monoclonal antibodies were amine-coupled to the research grade CM5 sensor chip of BIAcore 2000 (GE Healthcare). When binding of soluble candidate ligands for α9β1 was assessed, anti-V5 monoclonal antibody was coupled to the sensor chip and recombinant soluble α9β1 tagged with V5 sequence was passed over (20 μl /min) to be immobilized on the sensor chip.

Transwell migration- The undersides of polycarbonate membranes with 8 μm pores of Transwell (Corning) were coated with 15 μl of substrate at indicated concentrations. 1 x 10^5 of SW480 cells were added to the top of each chamber, then allowed to migrate to the lower chambers containing DMEM with 1% FBS at 37 ºC for 24 h in a humidified atmosphere with 5% CO_2. Migrated cells on the bottom side of the membrane were stained with crystal violet for counting.

Horizontal migration of neutrophils- Human neutrophils were isolated from peripheral blood by Ficoll-Hypaque density gradient centrifugation followed by 3% dextran sedimentation. Migration was assessed using TAXIScan (GE Healthcare Japan) with an etched silicon substrate and a flat glass plate which together formed a horizontal, 5-μm-deep microchannel (22). Neutrophils in channels were tracked by time-lapse photography and the number of cells was counted automatically. When blocking antibody was used, neutrophils were pre-incubated on ice for 15 min with antibody. A total of 5 x 10^3 neutrophils were applied to an edge of the microchannel in one compartment of the chamber with RPMI. To start the assay, 1 μl polymeric OPN (20 μg/ml), intact OPN (20 μg/ml), or fMLP (10^{-7} M) was injected into the opposite compartment with RPMI to form a gradient in the channel.

Results

Recombinant polymeric and monomeric osteopontin proteins- Anion-exchange chromatography of recombinant polymerized OPN is shown in Fig. 2A. To exclude non-polymerized OPN seen in lane 1-3, fractions of lane 4-11 were collected. Purity of the polymeric OPN, intact monomeric OPN and thrombin-cleaved nOPN were confirmed by western blotting with mAb HUC750 (Fig. 2B). HUC750 reacted polymeric OPN, intact monomeric OPN and thrombin-cleaved nOPN, and showed these OPN proteins were uncontaminated. 'Intact OPN' represents intact (full-length) monomeric OPN hereafter.

Cell adhesion to polymeric osteopontin- To investigate whether integrin α9β1 really acts as a receptor for polymeric OPN we first examined cell adhesion. α9-transfected SW480 cells, which express α9β1 in addition to two naturally expressed polymeric OPN-binding integrins, α5β1 and αvβ5 (9), were used as previously described (4). Both mock- and α9-transfected SW480 cells adhered well to polymeric OPN (Fig. 3A). However, adhesion of mock-transfectants was significantly reduced in the presence of anti-α5β1 and anti-αvβ5 antibodies, whereas adhesion of α9-transfected cells was only slightly inhibited. Anti-α9β1 partially inhibited adhesion of α9-transfected cells. When these mAbs against α5β1, αvβ5 and α9β1 were used in combination, adhesion of α9-transfectants was dramatically reduced. These results indicate α9β1 mediates cell adhesion to polymeric OPN in addition to α5β1 and αvβ5. Next, we examined adhesion to intact OPN and thrombin-cleaved nOPN, non-ligand and ligand for α9β1, respectively, as control experiments. Mock- and α9-transfected SW480 cells showed modest, comparable levels of adhesion to intact OPN, which was completely abrogated by the combination of anti-α5β1 and anti-αvβ5, whereas anti-α9β1 had no effect (Fig. 3B, left). For thrombin-cleaved nOPN, patterns of adhesion of mock- and α9-transfected SW480 cells in the presence or absence of antibodies was essentially the same as to polymeric OPN (Fig. 3B right). The loss of adhesion with anti-α5β1 and anti-αvβ5 to intact OPN, and contrasting adhesion to throm-

bin-cleaved nOPN validates our experimental system and increases confidence that α9β1-mediates cell adhesion to polymeric OPN.

Cell migration to polymeric osteopontin- We next assessed α9β1-mediated cell migration to polymeric OPN in a transwell migration assay. Fig. 4A shows pictures of the under side of Transwell membrane. Stained α9-transfected SW480 cells transmigrated onto the under side of membrane coated with intact OPN or polymeric OPN appear as dark dots. The obvious difference illustrates that α9-transfectants migrate in response to polymeric OPN but not to intact OPN. To confirm this enhanced migration is α9β1-mediated, we analyzed the migration in the presence and absence of anti-OPN-receptor-integrin antibodies (Fig. 4B). Compared to intact OPN, both mock- and α9-transfected cells migrated onto polymeric OPN, with enhanced migration in α9-transfectants. Migration of the mock-transfectants was inhibited by a combination of antibodies against α5β1 and αvβ5, whereas the inhibitory effect of the same combination on α9-transfectants was minimal. However, migration of the α9-transfectants was dramatically inhibited by addition of anti-α9β1. These results indicate that α9β1 mediates migration onto polymeric OPN.

Direct binding of α9β1 to polymeric osteopontin- The α9β1-mediated cell adhesion and migration to polymeric OPN strongly suggest that polymeric OPN is a ligand for α9β1. We next detected direct binding of α9β1 to polymeric OPN. First, binding activity of recombinant α9β1 was analyzed with affinity chromatography over affinity matrices coupled with TNfn3RAA, a well-characterized α9β1-specific ligand (17). Two bands in the elution fractions in Fig. 5A (lane 2-4) correspond to biotin-labeled α9β1 that was eluted with EDTA, indicating that the recombinant heterodimer retains expected cation-dependent ligand binding function. Recombinant α9β1 was incubated in wells of ELISA plates coated with polymeric OPN, intact OPN, TNfn3RAA or vitronectin, an irrelevant integrin ligand. α9β1 bound to polymeric OPN as well as TNfn3RAA in a dose-dependent manner in the presence of Ca^{2+}/Mg^{2+} or Mn^{2+} (Fig. 5B left and middle). No binding to intact OPN or vitronectin in the same condition confirmed the specificity of recombinant α9β1. When the divalent cations were depleted and EDTA was present, bindings of α9β1 to polymeric OPN and TNfn3RAA were completely abolished at all concentrations (Fig. 5B, right). To further explore binding of soluble α9β1 to polymeric OPN, we next performed SPR analysis, with recombinant α9β1 coupled to the instrument's sensor chip. Response unit curves at 3, 10, 30, and 90 μg/ml of polymeric OPN clearly illustrate dose-dependent binding of polymeric OPN to α9β1 (Fig. 5C). α9β1-OPN complex appeared to dissociate easily as expected for integrin-ligand interactions as demonstrated by the sharp decline in binding at 180 sec, when polymeric OPN is no longer present in the running buffer. These results of binding assays with soluble or immobilized α9β1 indicate that integrin α9β1 specifically binds to polymeric OPN.

Integrin α9β1 mediates neutrophil migration to polymeric osteopontin- To explore biological meaning of this receptor-ligand interaction, we next evaluated migration of neutrophils, because α9β1 is highly expressed on neutrophils and found to mediate neutrophil migration to VCAM-1 (14). Further, thrombin-cleaved nOPN, a ligand for α9β1, was also reported to attract neutrophils. Images of neutrophils migrating through a horizontal, 5-μm-deep microchannel containing a gradient of a chemoattractant were captured with time-lapse microscopy and the numbers of neutrophils in the channel were counted automatically. Fig. 6A shows the number of neutrophils that migrated into a channel with gradient of polymeric (Video1) or intact OPN over a period of 60 min. A blocking antibody to α9β1 partially, but clearly, inhibited the migration (Video2), which was in contrast to the lack of inhibition seen with anti-β2 antibody. Consistently with the previous report, only minimal directed migration was seen in the presence of a gradient of intact, monomeric OPN (Video3). In a gradient of fMLP (Fig. 6B), neutrophils also migrated (Video4), but this effect was not blocked by anti-α9β1 but was partially blocked by anti-β2 (23). In the presence of PBS in both upper and lower panels, there were slight increases in the number of cells over time, which can be attributed to random migration. Neutrophils migrating through the channels can be seen in the images shown in Fig 6C. At 0 min, neutrophils were aligned at the upper edge of the channel. After 60 minutes cells gradually migrated into higher concentrations of polymeric OPN, but not into higher concentrations of intact OPN. Fig. 6D shows the number of cells that migrated per minute into the chamber in a gradient of polymeric OPN, in the presence or absence of antibodies against α9β1 and β2, during the first 10 min of the experiment, when the migration curves were linear (Fig. 6A). The difference in rates of migration

under these conditions shows that anti-α9β1, in contrast to anti-β2, significantly inhibited neutrophil migration to polymerized OPN.

Integrin α9β1 recognizes a site other than SVVYGLR in polymeric osteopontin- At the beginning of the present study, we hypothesized α9β1 should bind to polymeric OPN by recognizing the SVVYGLR site in the same manner to bind to thrombin-cleaved nOPN. The aim of the final part of our investigation was to test this hypothesis. First, we abolished the binding capacity of the SVVYGLR domain by two mutations, which we had previously shown completely abrogate α9β1-mediated adhesion to thrombin-cleaved nOPN (5), dYGLR and Y165A, in which YGLR was deleted and where Y was replaced with A, respectively. Although the mutations disrupted the cell adhesive property of thrombin-cleaved nOPN, α9-transfected SW480 cells adhered equally well to wild type or mutated polymeric OPNs (Fig 7A). Binding of recombinant α9β1 to polymeric OPN with either mutation was also the same as that seen for wild type polymeric OPN (Fig. 7B), again indicating that integrin α9β1 recognizes a sequence different from SVVYGLR. To evaluate whether these results were due to exposure of a non-SVVYGLR recognition site(s) on polymeric OPN with greater affinity than the SVVYGLR domain or whether SVVYGLR was not exposed on polymeric OPN, we examined the binding of SVVYGLR specific antibody 34E3 to polymeric OPN. Binding of 34E3 to thrombin-cleaved nOPN-coated wells was completely abolished in the presence of SVVYGLR peptide, but not by GVRSVLY scrambled peptide (Fig 8A), confirming that 34E3 recognizes and binds specifically to the SVVYGLR sequence. However, 34E3 did not bind to either polymeric OPN or intact OPN, whereas a control OPN antibody HUC750 bound equally well to all three forms of OPN tested (Fig 8B). These findings were also confirmed by SPR analysis. Again, polymeric OPN as well as intact OPN did not bind to 34E3 on the sensor chip, whereas thrombin-cleaved nOPN obviously bound 34E3 (Fig. 8C). These results indicate that integrin α9β1 binds to polymeric OPN at a site distinct from SVVYGLR, and that the SVVYGLR sequence remains cryptic in polymeric OPN, just as it is in intact monomeric OPN.

Discussion

In the present study we have found that polymerization of OPN results in a new interaction with the α9β1 integrin, that this interaction induces neutrophil migration, and that α9β1 binds to a site distinct from SVVYGLR, the previously described recognition sequence in thrombin-cleaved OPN. These results demonstrated that OPN changes its property upon polymerization at least in part by means of a new molecular interaction. TG2 catalyzed polymerization of OPN was first identified *in vitro* in 1991 (10). Recently *in vivo* polymerization was demonstrated by western blotting of a high molecular weight form (12) (13) and by N-terminal sequence (12). Because ligand density and affinity are major determinants of integrin clustering, and polymerization increases local density of integrin-binding sequences, it is conceivable that polymerization augments interaction of cells with OPN. We have in fact previously reported that integrin-mediated cell adhesion, spreading, and migration were enhanced by polymeric OPN associated with intense focal contact formation (9). In the present study, we have identified a new molecular interaction of polymeric OPN and demonstrated at least one physiological consequence – neutrophil chemotaxis.

TG2 is known to modulate cell-matrix interaction by cross-linking several extracellular matrix proteins, including collagen, laminin and fibronectin, effects generally thought to stabilize tissue integrity (11, 16). In addition, since cross-linking changes physical and chemical properties of a protein, polymerization could cause conformational changes in these or other proteins that result in new molecular interactions (16).

Injection of intact OPN has been demonstrated to induce neutrophil recruitment by independent groups in mice and rats (24, 25). Further, a OPN-neutralizing antibody inhibited neutrophil infiltration into livers in mice with concanavalin A (ConA)- or lipopolysaccharide (LPS) -induced hepatitis (26, 27). It is thus clear that OPN contributes to neutrophils *in vivo*. On the other hand, as we have found, there is little evidence for any chemotactic activity of native monomeric OPN *in vitro*. In contrast, both thrombin-cleaved nOPN (31) and, in the current study, polymerized OPN, are potent neutrophil chemoattractants. It is thus conceivable that injected or endogenously produced OPN recruits neutrophils as a consequence of one of these post-translational modifications. The only report that claimed to show *in vitro* migration of neutrophils to native

OPN used OPN purified from a macrophage cell line, RAW 264.7 cells (24), a condition that would be susceptible to both thrombin-cleavage and TG2-mediated polymerization. It is noteworthy that these two different post-translational modifications render OPN accessible to binding to the same receptor, α9β1.

The totally unaffected adhesion and binding of α9-ransfectants and recombinant α9β1 to polymeric OPN with disrupted SVVYGLR sequence demonstrated that SVVYGLR in polymeric OPN is not a recognition site of α9β1. Furthermore, the absence of binding of SVVYGLR-specific antibody to polymeric OPN suggest that the SVVYGLR sequence is not even exposed on the surface of the polymer. We are not certain why two different post-translational modifications of OPN, cleavage and polymerization, result in employment of the same receptor through distinct binding sites. Nonetheless, integrin α9β1 appears to be critical for chemotactic responses of neutrophils to OPN.

One important role for the interaction of α9β1 with polymerized OPN might be to concentrate neutrophils at sites of OPN- polymerization, ensuring that their immune products and activities remain at this site, while minimizing unnecessary injury to the other sites. Since both OPN and TG2 are upregulated at sites of injury and inflammation, it is conceivable that polymeric OPN could be generated in response to injury. Thrombin-cleaved nOPN could also be generated at sites of inflammation so it will be important to investigate the kinetics and location of these two post-translational modifications under various conditions *in vivo* and the relative contribution of each to neutrophil recruitment and/or retention.

In conclusion, we have identified a *de novo* molecular interaction upon polymerization of OPN and concomitant induction of neutrophil migration. Our findings illustrate that OPN gains a new function through polymerization, and open new avenues to understand the biological significance of OPN-polymerization and its potential role in regulating tissue inflammation.

References

1. Denhardt, D.T., M. Noda, A.W. O'Regan, D. Pavlin, and J.S. Berman. 2001. Osteopontin as a means to cope with environmental insults: regulation of inflammation, tissue remodeling, and cell survival. *J. Clin. Invest.* 107:1055-1061.
2. Scatena, M., L. Liaw, and C.M. Giachelli. 2007. Osteopontin. A multifunctional molecule regulating chronic inflammation and vascular disease. *Arterioscler. Thromb. Vasc. Biol* 27:2302-2309.
3. McAllister, S., A. Gifford, A. Greiner, S. Kelleher, M. Saelzler, T. Ince, F. Reinhardt, L. Harris, B. Hylander, E. Repasky, and R. Weinberg. 2008. Systemic endocrine instigation of indolent tumor growth requires osteopontin. *Cell* 133:994-1005.
4. Yokosaki, Y., K. Tanaka, F. Higashikawa, K. Yamashita, and A. Eboshida. 2005. Distinct structural requirements for binding of the integrins αvβ6, αvβ3, αvβ5, α5β1 and α9β1 to osteopontin. *Matrix Biol.* 24:418-427.
5. Yokosaki, Y., N. Matsuura, T. Sasaki, I. Murakami, H. Schneider, S. Higashiyama, Y. Saitoh, M. Yamakido, Y. Taooka, and D. Sheppard. 1999. The integrin α9β1 binds to a novel recognition sequence (SVVYGLR) in the thrombin-cleaved amino-terminal fragment of osteopontin. *J. Biol. Chem.* 274:36328-36334.
6. Yokosaki, Y., H. Monis, J. Chen, and D. Sheppard. 1996. Differential effects of the integrins α9β1, αvβ3, and αvβ6 on cell proliferative responses to tenascin. Roles of the beta subunit extracellular and cytoplasmic domains. *J Biol Chem* 271:24144-24150.
7. Senger, D., C. Perruzzi, S. Papadopoulous, and L. Van de Water. 1994. Adhesive properties of osteopontion: regulation by a naturally occurring thrombin-cleavage in close proximity to the GRDGS cell-binding domain. *Mol. Biol. Cell* 5:565-574.
8. Agnihotri, R., H.C. Crawford, H. Haro, L.M. Matrisian, M.C. Havrda, and L. Liaw. 2001. Osteopontin, a novel substrate for matrix metalloproteinase-3 (stromelysin-1) and matrix metalloproteinase-7 (matrilysin). *J Biol Chem* 276:28261-28267.
9. Higashikawa, F., A. Eboshida, and Y. Yokosaki. 2007. Enhanced biological activity of polymeric osteopontin. *FEBS Lett* 581:2697-26701.

10. Prince, C., D. Dickie, and C. Krumdieck. 1991. Osteopontin, a substrate for transglutaminase and factor XIII activity. *Biochem. Biophys. Res. Commun.* 177:1205-1210.
11. Lorand, L., and R. Graham. 2003. Transglutaminases: crosslinking enzymes with pleiotropic functions. *Nat. Rev. Mol. Cell Biol.* 4:140-156.
12. Kaartinen, M.T., S. El-Maadawy, N.H. Rasanen, and M.D. McKee. 2002. Tissue transglutaminase and its substrates in bone. *J. Bone Miner. Res.* 17:2161-2173.
13. Kaartinen, M.T., M. Murshed, G. Karsenty, and M.D. McKee. 2007. Osteopontin Upregulation and Polymerization by Transglutaminase 2 in Calcified Arteries of Matrix Gla Protein-deficient Mice. *J Histochem Cytochem* 55:375-386.
14. Taooka, Y., J. Chen, T. Yednock, and D. Sheppard. 1999. The integrin α9β1 mediates adhesion to activated endothelial cells and transendothelial neutrophil migration through interaction with vascular cell adhesion molecule-1. *J Cell Biol* 145:413-420.
15. Smith, L.L., H.K. Cheung, L.E. Ling, J. Chen, D. Sheppard, R. Pytela, and C.M. Giachelli. 1996. Osteopontin N-terminal domain contains a cryptic adhesive sequence recognized by a9b1 integrin. *J. Biol. Chem.* 271:28485-28491.
16. Zemskov, E.A., A. Janiak, J. Hang, A. Waghray, and A.M. Belkin. 2006. The role of tissue transglutaminase in cell-matrix interactions. *Frontiers in Bioscience* 11:1057-1076.
17. Yokosaki, Y., E.L. Palmer, A.L. Prieto, K.L. Crossin, M.A. Bourdon, R. Pytela, and D. Sheppard. 1994. The integrin α9β1 mediates cell attachment to a non-RGD site in the third fibronectin type III repeat of tenascin. *J. Biol. Chem.* 269:26691-26696.
18. Wang, A., Y. Yokosaki, R. Ferrando, J. Balmes, and D. Sheppard. 1996. Differential regulation of airway epithelial integrins by growth factors. *Am J Respir Cell Mol Biol* 15:664-672.
19. Takahashi, H., T. Isobe, S. Horibe, J. Takagi, Y. Yokosaki, D. Sheppard, and Y. Saito. 2000. Tissue transglutaminase, coagulation factor XIII, and the pro-polypeptide of von Willebrand factor are all ligands for the integrins α9β1 and α4β1. *J Biol Chem* 275:23589-23595.
20. Sato, Y., N. Nishimichi, A. Nakano, K. Takikawa, N. Inoue, H. Matsuda, and T. Sawamura. 2008. Determination of LOX-1-ligand activity in mouse plasma with a chicken monoclonal antibody for ApoB. *Atherosclerosis* 200: 303-309.
21. Yokosaki, Y., N. Matsuura, S. Higashiyama, I. Murakami, M. Obara, M. Yamakido, N. Shigeto, J. Chen, and D. Sheppard. 1998. Identification of the ligand binding site for the integrin α9β1 in the third fibronectin type III repeat of tenascin-C. *J Biol Chem* 273:11423-11428.
22. Nitta, N., T. Tsuchiya, A. Yamauchi, T. Tamatani, and S. Kanegasaki. 2007. Quantitative analysis of eosinophil chemotaxis tracked using a novel optical device -- TAXIScan. *J Immunol Methods* 320:155-163.
23. Carrigan, S., D. Pink, and A. Stadnyk. 2007. Neutrophil transepithelial migration in response to the chemoattractant fMLP but not C5a is phospholipase D-dependent and related to the use of CD11b/CD18. *J Leukoc Biol* 82:1575-1584.
24. Koh, A., A.P.B.d. Silva, A.K. Bansal, M. Bansal, C. Sun, H. Lee, M. Glogauer, J. Sodek, and R. Zohar. 2007. Role of osteopontin in neutrophil function. *Immunology* 122:466-475.
25. Banerjee, A., U. Apte, R. Smith, and S. Ramaiah. 2006. Higher neutrophil infiltration mediated by osteopontin is a likely contributing factor to the increased susceptibility of females to alcoholic liver disease. *J Pathol* 208:473-485.
26. Diao, H., S. Kon, K. Iwabuchi, C. Kimura, J. Morimoto, D. Ito, T. Segawa, M. Maeda, J. Hamuro, T. Nakayama, M. Taniguchi, H. Yagita, L.V. Kaer, K. Onoe, D. Denhardt, S. Rittling, and T. Uede. 2004. Osteopontin as a Mediator of NKT Cell Function in T Cell-Mediated Liver Diseases. *Immunity* 21:539-550.
27. Apte, U.M., A. Banerjee, R. McRee, E. Wellberg, and S.K. Ramaiah. 2005. Role of osteopontin in hepatic neutrophil infiltration during alcoholic steatohepatitis. *Toxicol Appl Pharmacol* 207:25-38.

Footnotes

*We thank Drs. Dean Sheppard (UCSF) and Yuji Saito (Tokyo Institute for Technology, Japan) for the transfectants, antibody and guinea pig TG2. We also thank the Research Center for Molecular Medicine and Analysis Center of Life Science, Hiroshima University, for the use of facilities. This work was supported in part by a grant from Japan New Energy and Industrial Technology Development Organization (to N.N., Y.T., H.M. and Y.Y., New functional antibody technologies) and by a grant from Tsuchiya Memorial Medical Foundation (to Y.Y.)

§These authors contributed equally to this work

¶Current address: Department of Molecular Nutrition Sciences, Graduate School of Biomedical Sciences, Hiroshima University, 1-2-3 Kasumi, Minamiku, Hiroshima, 734-8551, Japan.

The abbreviations used are: OPN, osteopontin; TG2, transglutaminase 2; nOPN, N-terminal fragment of osteopontin; mAb, monoclonal antibody; HRP, horse radish peroxidase; TNfn3RAA, tenascin-C fragment of third fibronectin type III repeat containing alanine substitution mutations in the RGD site; SPR, surface plasmon resonance.

Figure legends

Fig. 1 Schematic diagram of OPN and. Two integrin binding sites (boxed), a thrombin-cleavage site (arrowed), and a putative transglutamination site (circled) are shown. A term thrombin-cleaved nOPN is defined as in the figure.

Fig. 2 Recombinant OPNs used in this study. (A) A silver-stained gel for fractions of anion exchange chromatography. Fractions containing low *Mr* (< 50 kDa) OPN were excluded. (B) Western blot of purified polymeric OPN (lane 1), intact OPN (lane 2), and thrombin-cleaved nOPN (lane 3) probed with mAb HUC750.

Fig. 3 Integrin α9β1-mediated cell adhesion to polymeric OPN. (A) Adhesion of mock- or α9-transfected SW480 cells to polymeric OPN is shown as O.D. (B) O.D. expresses for adhesion of mock- or α9-transfected SW480 cells to intact OPN and thrombin-cleaved nOPN. The presence or absence of antibodies against α5β1, αvβ5, and α9β1 is indicated below. Values represent the mean + SD of triplicate wells collected in three independent experiments (n=9).

Fig. 4 Integrin α9β1-mediated cell migration to polymeric OPN. (A) Micrograph of the underside of membranes of Transwell. α9-transfected SW480 cells are stained which migrated through the membrane coated with 15 μl of 10 μg/ml intact or polymeric OPN. Bars represent 100 μm. (B) Number of mock- and α9-transfected SW480 cells migrated to intact or polymeric OPN in the presence or absence of antibodies against α5β1, αvβ5, and α9β1 as indicated below. Values represent the mean + SD of three independent experiments where cell number was counted in three randomly selected fields (n=9).

Fig. 5 Binding of recombinant α9β1 to polymeric OPN. (A) Affinity chromatography. Biotin-labeled recombinant α9β1 was passed over TNfn3RAA-coupled Sepharose column. Bound protein was eluted with 20 mM EDTA and analyzed by 7.5% polyacrylamide gel under non-reducing conditions. The final fraction washed with column buffer was in lane 1, elution fractions (one column volume x 3) were in lanes 2-4. The positions of *Mr* markers (in kDa) are shown to the left. (B) Recombinant α9β1 (2 μg/ml) in Tris-buffered saline containing 1 mM Ca^{2+} and 1 mM Mg^{2+}, 1mM Mn^{2+}, or EDTA, as indicated, was allowed to bind to wells of ELISA plate coated with 0.1-30 μg/ml of polymeric OPN, TNfn3RAA, or vitronectin. To detect α9β1, then anti-V5 mAb was placed in wells followed by secondary antibody and colorimetry. Values represent mean + SD of duplicate wells in three independent experiments (n=6). (C) Surface plasmon resonance (Biacore) analysis of recombinant α9β1-binding to polymeric OPN. The

vertical axis shows the surface plasmon resonance intensity in resonance units (RU). The horizontal axis shows duration of flow of buffer containing 1 mM Mn^{2+}. Recombinant α9β1 (10 μg/ml) was bound to anti-V5 that had been coupled to the sensor chip. Polymeric OPN at a concentration of 3, 10, 30, or 90 μg/ml in buffer was added over the sensor chip at a flow rate of 10 μl/min for 180 s.

Fig. 6 Neutrophil migration to polymeric OPN. (A) Numbers of neutrophils that had migrated into and were present within the five-micron horizontal channels containing gradients of polymeric OPN (upper panel), or fMLP (lower panel) at each time point during 60 min. Neutrophils were pre-incubated in the presence or absence of antibodies as indicated at the right. (B) Micrographs of the channels containing gradients intact OPN or polymeric OPN taken at 0 and 60 minutes. Rectangles seen at top and bottom of the each image are the columns that support the channel. Neutrophils appear as small grey objects. Movies are provided as supplemental figures. (C) Rate of neutrophil migration toward polymeric OPN in the presence or absence of antibodies. Values represent the average number of cells migrating per minute into a channel for the first 10 min of the experiment and are the mean + SD of three independent experiments (n=3). ** Indicates $p<0.01$ from no antibody by student's *t*-test.

Fig. 7 The SVVYGLR-independent interaction of α9-transfected cells and recombinant α9β1 with polymeric OPN (A) Adhesion of α9-transfected SW480 cells to polymeric OPN and thrombin-cleaved nOPN having a wild-type (white columns) or mutated SVVYGLR sequence (gray columns); dYGLR and Y165A represent mutants in which YGLR is deleted and Y is replaced with A in the SVVYGLR sequence, respectively. Cells were plated in wells coated with 5 μg/ml of substrate in the presence of anti-α5β1 and -αvβ5. (B) Binding of recombinant α9β1 to wild type or mutated polymeric OPN and vitronectin (black column). Recombinant α9β1 was allowed to bind to coated substrates (5 μg/ml) in the presence of 1mM Mn^{2+}. To detect α9β1, then anti-V5 mAb was placed in wells followed by secondary antibody and colorimetry. Values represent mean + SD from three independent experiments with triplicate (n=9) wells.

Fig.8 Impaired recognition of polymeric OPN by SVVYGLR-specific antibody, 34E3 (A) Specificity of 34E3 was tested by incubating in wells coated with 5 μg/ml thrombin-cleaved nOPN in the presence or absence of 1 mg/ml SVVYGLR synthetic peptide or scrambled peptide, GVRSVLY. Fifty μl of 0.5 μg/ml mAb 34E3 was added to wells and incubated for 60 min followed by colorimetry with HRP-tagged secondary antibody. (B) Binding of 34E3 or control antibody HUC750 to polymeric OPN, intact OPN and thrombin-cleaved nOPN. Substrates were coated at 5 μg/ml. (C) Surface plasmon resonance analysis (Biacore) for binding of 34E3 to polymeric OPN, intact OPN and thrombin-cleaved nOPN. The three forms of OPNs were passed over the sensor chip to which 34E3 had been coupled at a flow rate of 20 μl/min. The vertical axis indicates SPR intensity (RU) and the horizontal axis shows the duration of flow of HBS buffer. (A), (B) Values represent mean + SD from three independent experiments with triplicate (A, B; n=9) wells. (C) Representative reaction curb form three independent experiments.

Legends for supplemental movies

Video1.mov Migration of neutrophils through 5 μm horizontal channel containing gradient of polymeric OPN. Time-lapse photographs taken for 60 min were compacted into 4-5 s.

Video2.mov Migration of neutrophils pretreated with anti-α9β1 mAb through 5 μm horizontal channel containing gradient of polymeric OPN. Time-lapse photographs taken for 60 min were compacted into 4-5 s.

Video3.mov Migration of neutrophils through 5 μm horizontal channel containing gradient of intact OPN. Time-laps photographs taken for 60 min were compacted into 4-5 s.

Video4.mov Migration of neutrophils through 5 μm horizontal channel containing gradient of fMLP. Time-lapse photographs taken for 60 min were compacted into 4-5 s.

Figure 1

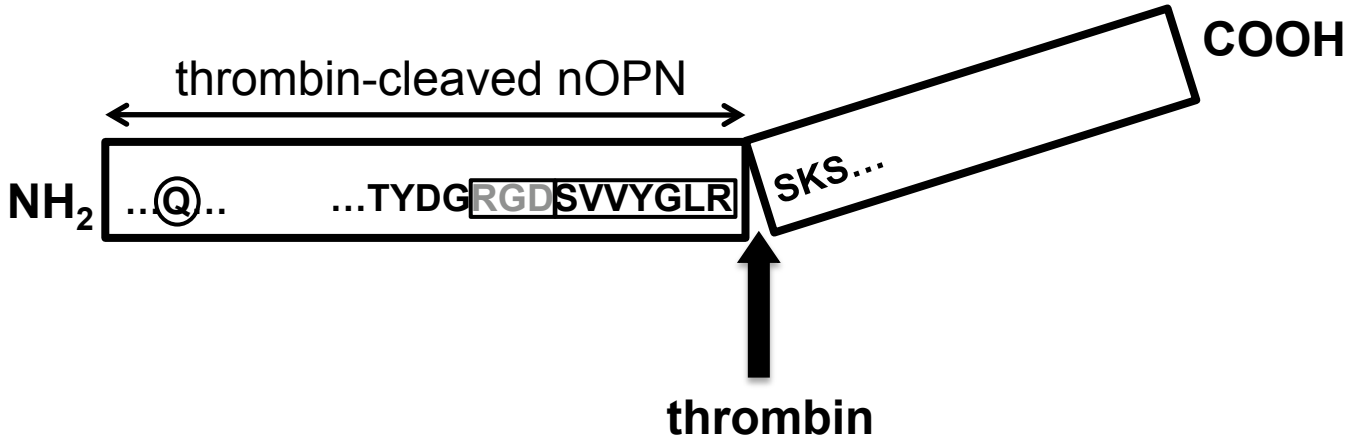
thrombin-cleaved nOPN
COOH
NH2
..Q..
...TYDGRGDSVVYGLR
SKS...
thrombin

Figure 2

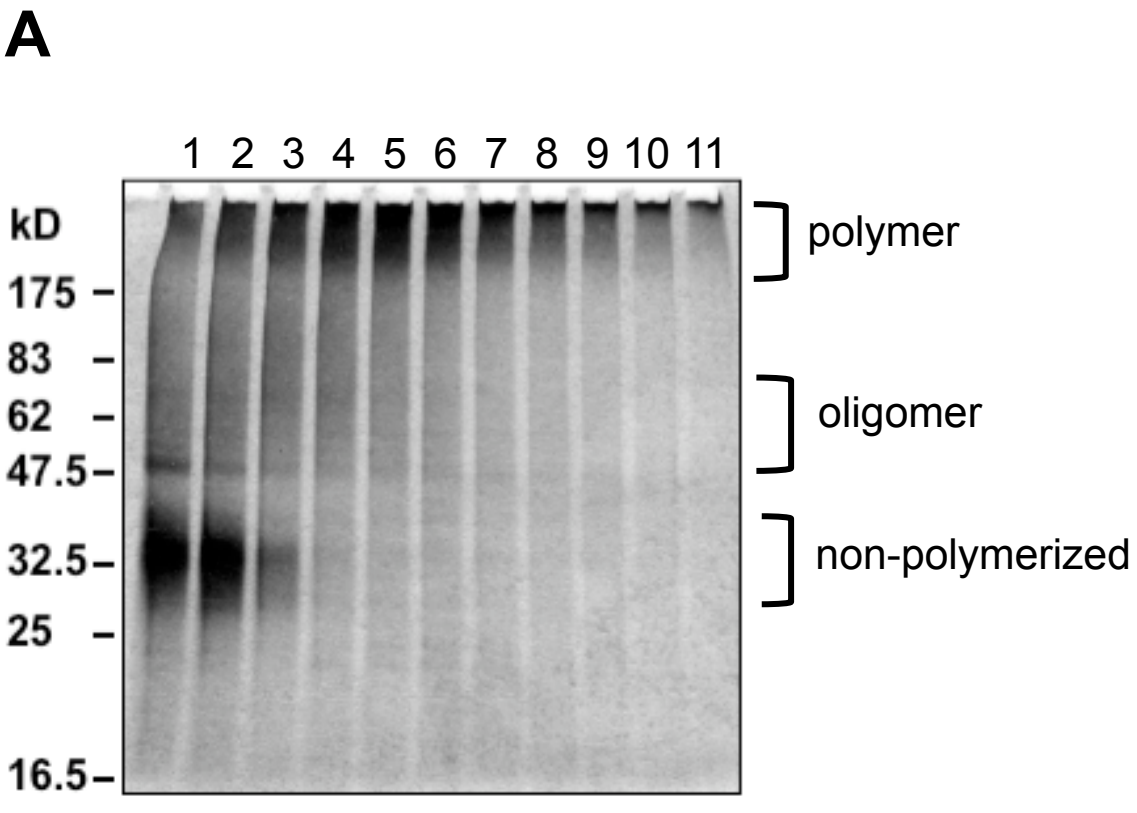
A
1 2 3 4 5 6 7 8 9 10 11
kD
175
83
62
47.5
32.5
25
16.5
polymer
oligomer
non-polymerized

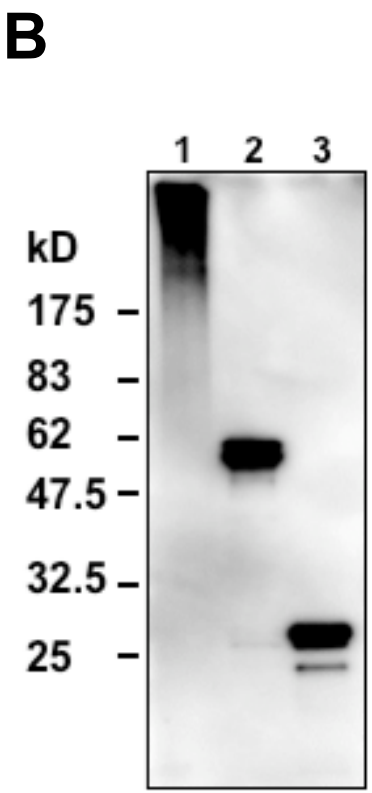
B
1 2 3
kD
175
83
62
47.5
32.5
25

Figure 3

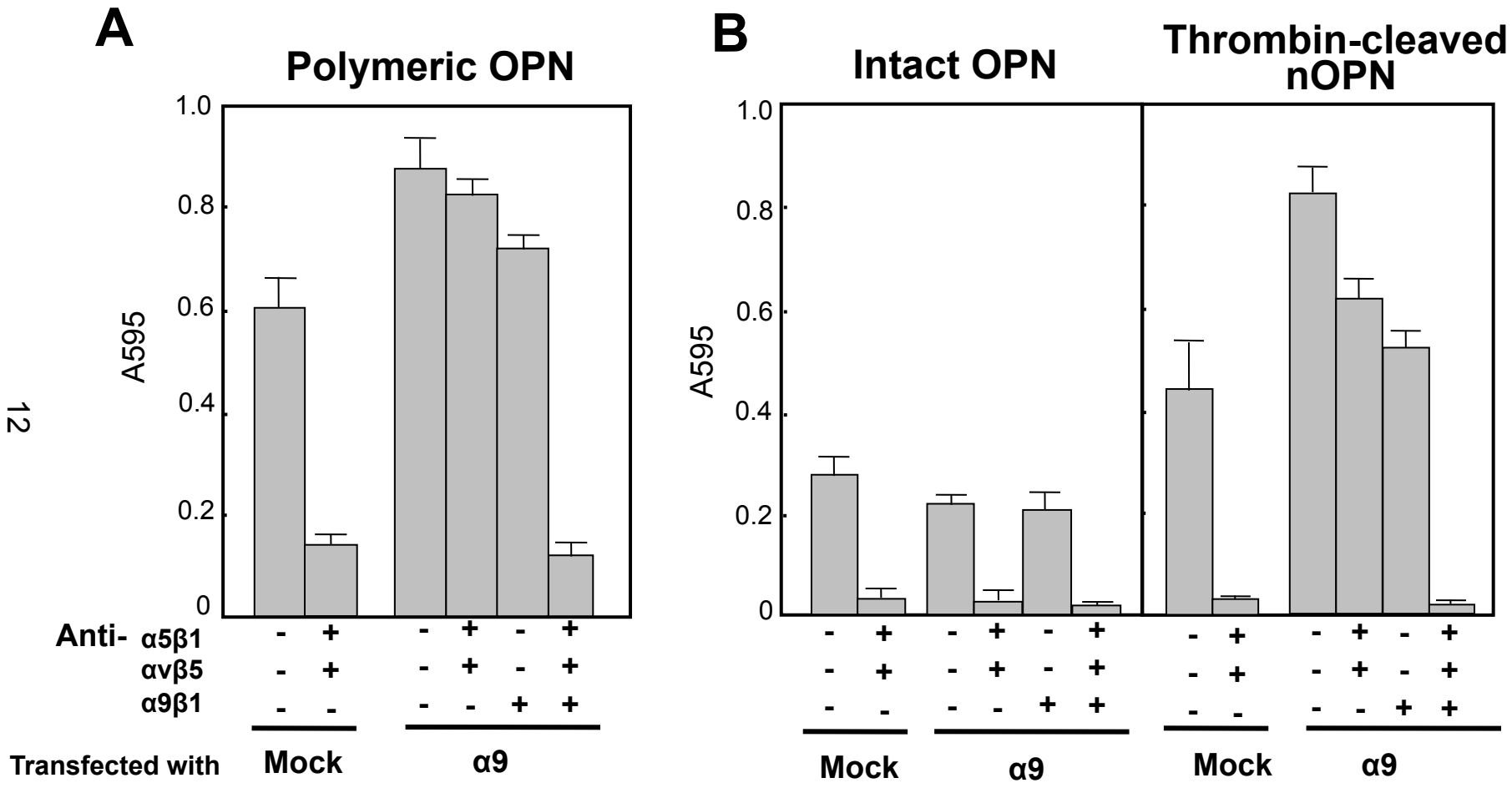
A
Polymeric OPN
B
Intact OPN
Thrombin-cleaved nOPN
A595
1.0
0.8
0.6
0.4
0.2
0
Anti- α5β1
αvβ5
α9β1
Transfected with
Mock
α9

Figure 4

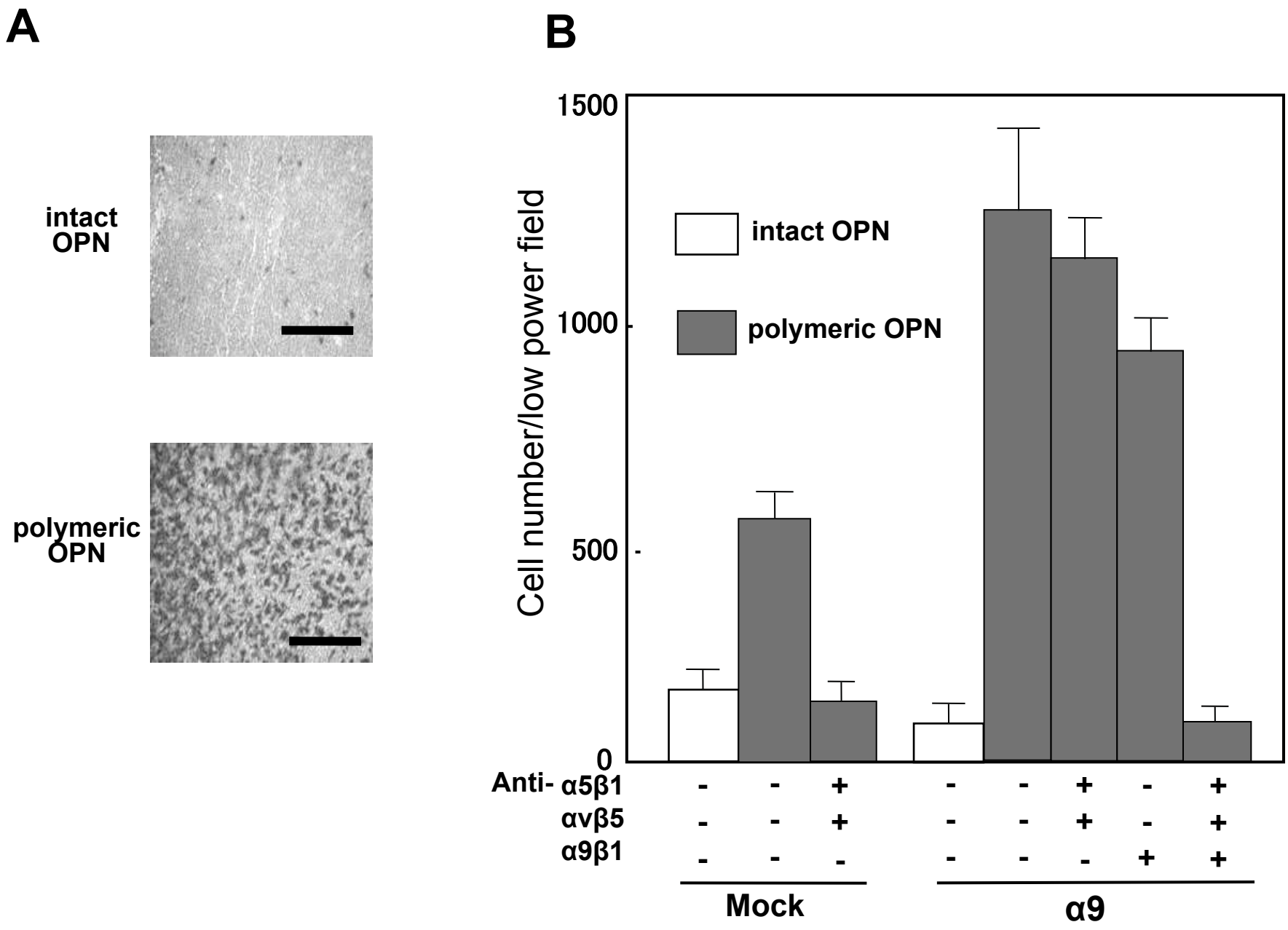
A
intact OPN
polymeric OPN
B
Cell number/low power field
1500
1000
500
0
intact OPN
polymeric OPN
Anti- α5β1
αvβ5
α9β1
Mock
α9

Figure 5

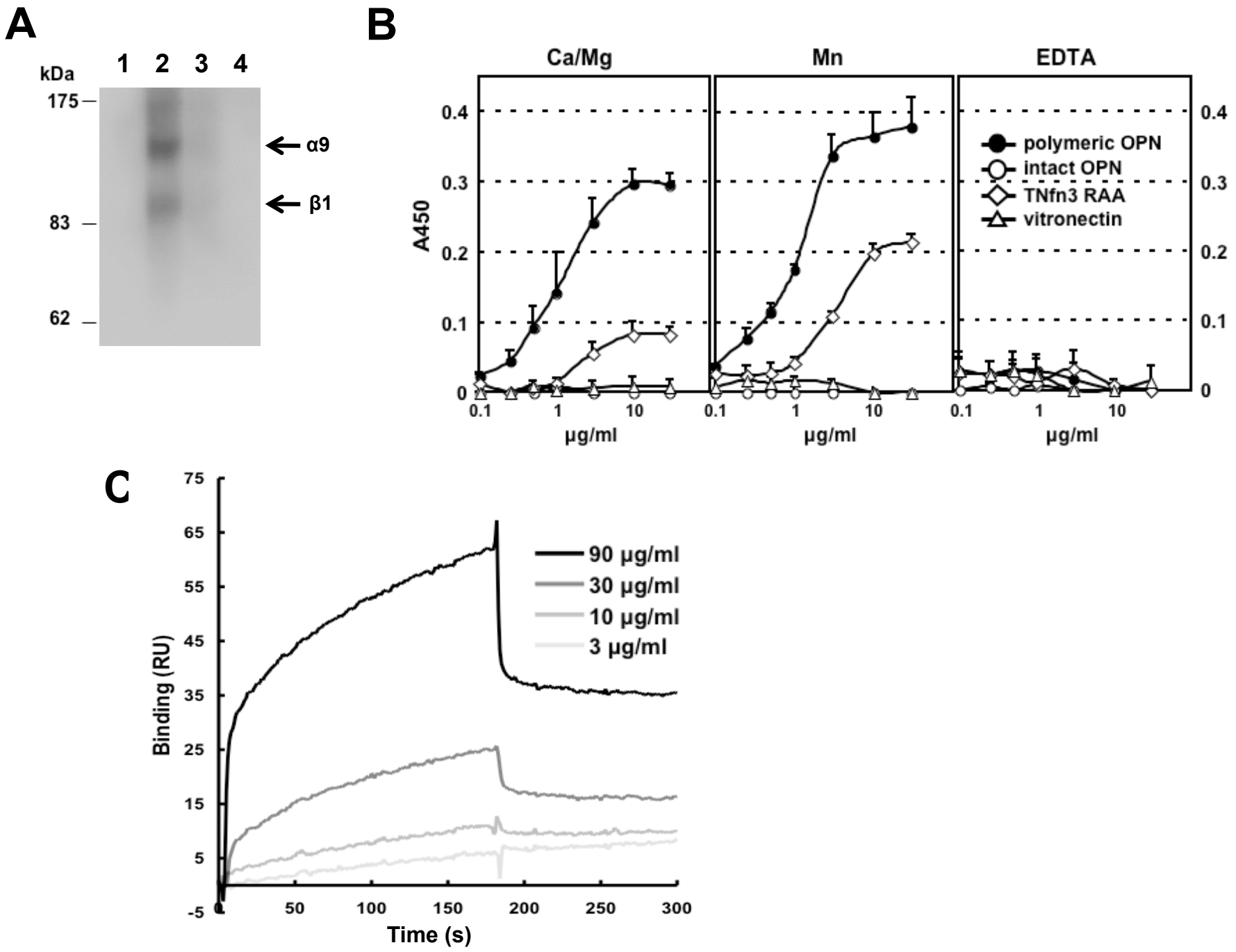
A
kDa
1 2 3 4
175
83
62
α9
β1
B
Ca/Mg
Mn
EDTA
A450
0.4
0.3
0.2
0.1
0
0.1
1
10
μg/ml
polymeric OPN
intact OPN
TNfn3 RAA
vitronectin
C
Binding (RU)
75
65
55
45
35
25
15
5
-5
50
100
150
200
250
300
Time (s)
90 μg/ml
30 μg/ml
10 μg/ml
3 μg/ml

Figure 6

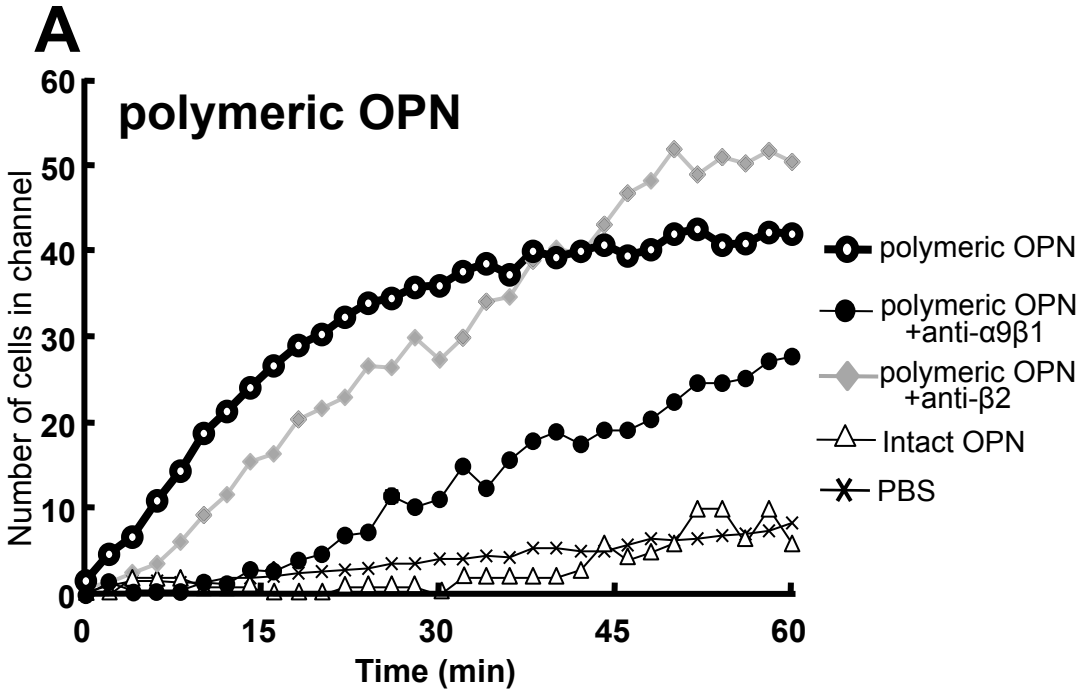
A
polymeric OPN
Number of cells in channel
Time (min)
polymeric OPN
polymeric OPN +anti-α9β1
polymeric OPN +anti-β2
Intact OPN
PBS

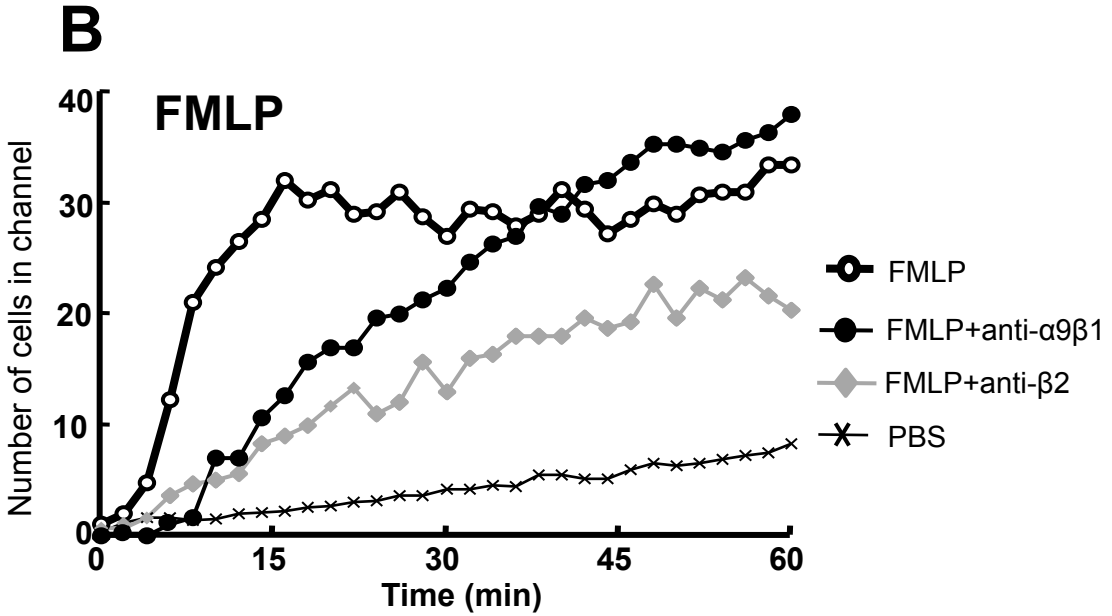
B
FMLP
Number of cells in channel
Time (min)
FMLP
FMLP+anti-α9β1
FMLP+anti-β2
PBS

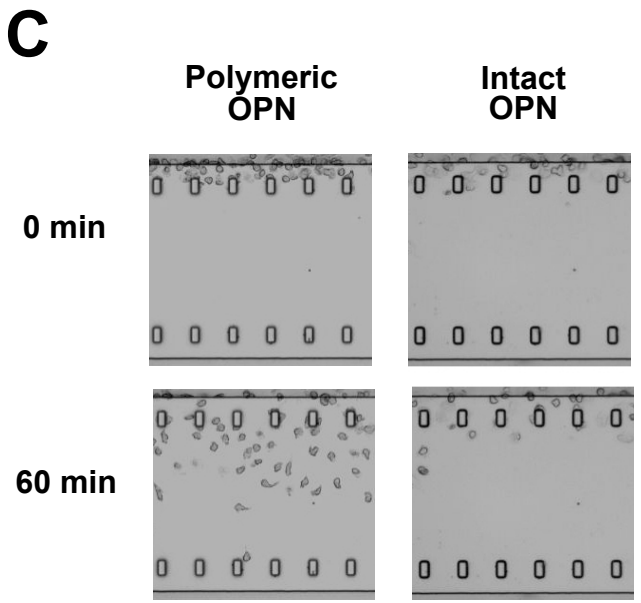
C
Polymeric OPN
Intact OPN
0 min
60 min

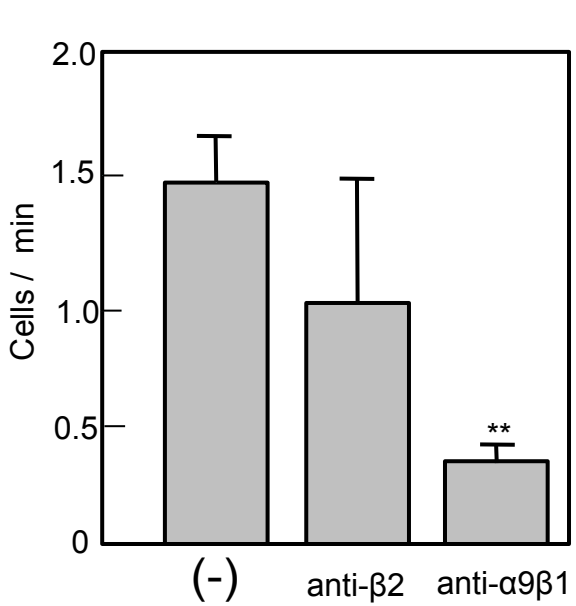
D
Cells / min
(-)
anti-β2
anti-α9β1
**

Figure 7

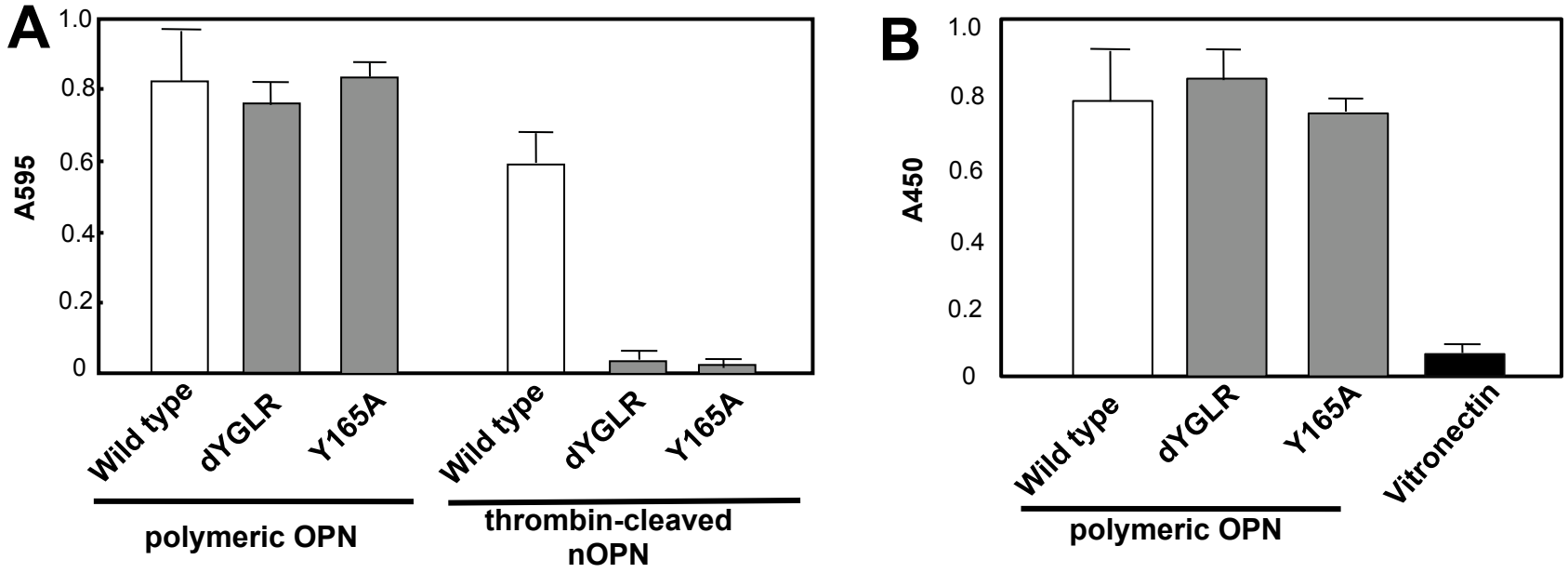
A
A595
1.0
0.8
0.6
0.4
0.2
0
Wild type
dYGLR
Y165A
Wild type
dYGLR
Y165A
polymeric OPN
thrombin-cleaved
nOPN
B
A450
1.0
0.8
0.6
0.4
0.2
0
Wild type
dYGLR
Y165A
Vitronectin
polymeric OPN

Figure 8

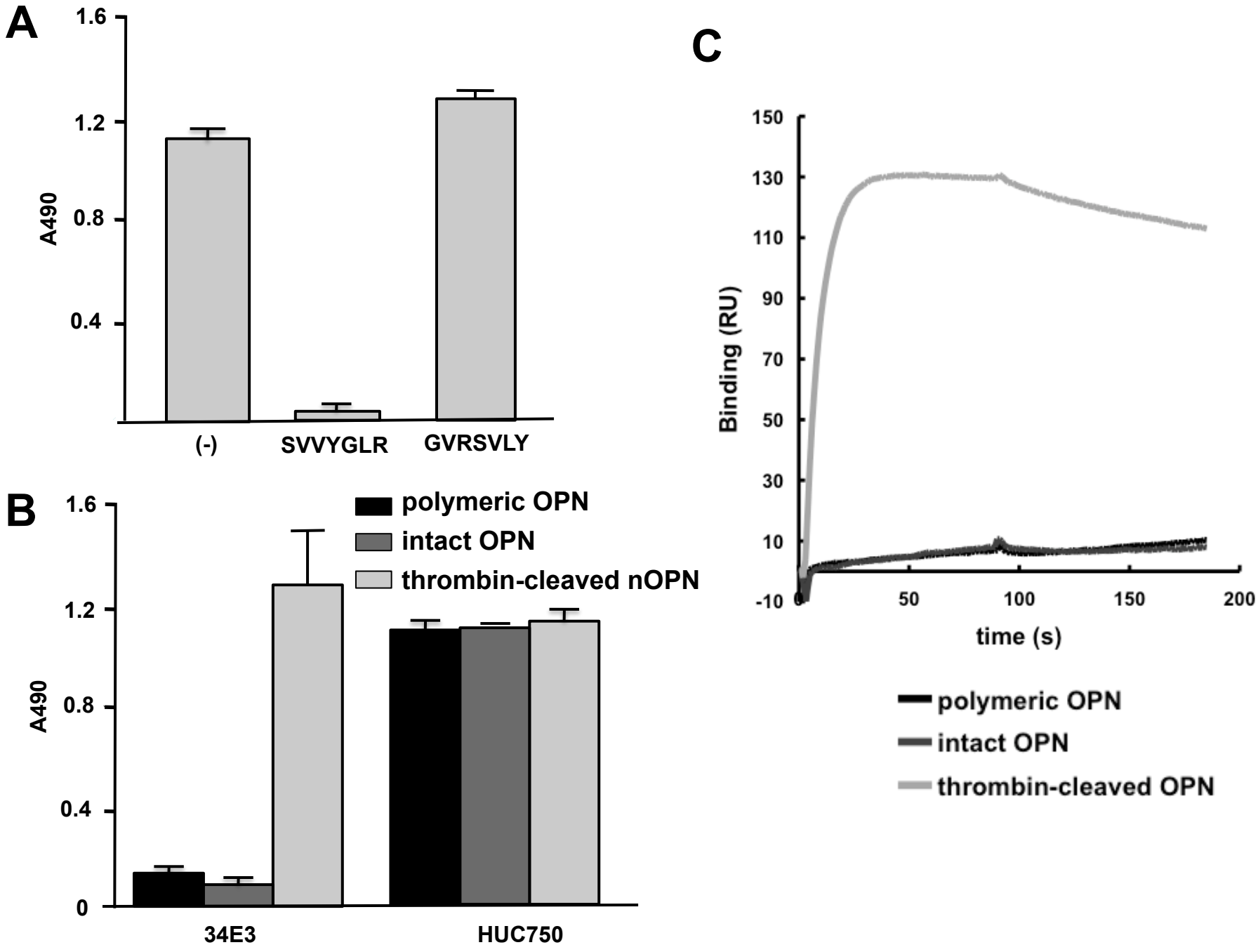
A
1.6
1.2
0.8
0.4
A490
(-)
SVVYGLR
GVRSVLY
B
polymeric OPN
intact OPN
thrombin-cleaved nOPN
1.6
1.2
0.8
0.4
0
A490
34E3
HUC750
C
150
130
110
90
70
50
30
10
-10
Binding (RU)
0
50
100
150
200
time (s)
polymeric OPN
intact OPN
thrombin-cleaved OPN